Rajamaki, Robin; Koivunen, Visa

Co-array Music under Angle-Independent Nonidealities

Published in:
Proceedings of 54th Asilomar Conference on Signals, Systems and Computers, ACSSC 2020

DOI:
10.1109/IEEECONF51394.2020.9443519

Published: 03/06/2021

Document Version
Peer reviewed version

Please cite the original version:
Rajamaki, R., & Koivunen, V. (2021). Co-array Music under Angle-Independent Nonidealities. In M. B. Matthews (Ed.), *Proceedings of 54th Asilomar Conference on Signals, Systems and Computers, ACSSC 2020* (pp. 230-235). [9443519] (Asilomar Conference on Signals, Systems, and Computers proceedings). IEEE. https://doi.org/10.1109/IEEECONF51394.2020.9443519

CO-ARRAY MUSIC UNDER ANGLE-INDEPENDENT NONIDEALITIES

Robin Rajamäki, and Visa Koivunen

Aalto University, Espoo, Finland

ABSTRACT

The difference co-array is crucial in determining the number of resolvable sources in direction-of-arrival (DoA) estimation. This virtual array of pairwise sensor position differences enables sparse arrays to identify vastly more sources than sensors. However, the idealized assumptions giving rise to the co-array, such as isolated omnidirectional gain patterns, may not hold in practice. Consequently, the applicability of the co-array model to real-world arrays needs to be investigated thoroughly. In this work, we consider a general class of angle-independent departures from the ideal model caused by nonideal sensors or compression of the array measurements. We study the impact of these nonidealities on DoA estimation using co-array MUSIC, assuming that the array is calibrated and that an infinite number of snapshots is available. We establish that proper use of the calibration data enables unbiased DoA estimation of more sources than sensors. Nonidealities may nevertheless cause subspace swap at low SNR.

1. INTRODUCTION

Direction-of-arrival (DoA) estimation is an important array processing task in diverse applications, such as communications, wireless localization, radar, sonar, and radio astronomy [1]. Especially subspace based high-resolution techniques have received a great deal of attention due to their ability to resolve closely spaced targets more accurately than traditional diffraction-limited methods. For example, the *multiple signal classification* (MUSIC) algorithm [2] can achieve comparable performance to the optimal maximum-likelihood estimation at a significantly lower computational cost. Under certain conditions, the estimation error of MUSIC approaches the Cramér-Rao bound as the sample size or signal-to-noise ratio (SNR) goes to infinity [3]. A variant of MUSIC, called *co-array MUSIC*, can also be used by N sensor sparse arrays to resolve $\mathcal{O}(N^2)$ sources [4, 5]. Co-array MUSIC leverages the structure of the set of pairwise sensor position differences, known as the *difference co-array*. The key advantage of the difference co-array is that it can have many more virtual elements than physical sensors and a uniform structure even when the physical array is nonuniform.

A limitation of MUSIC is that it requires precise knowledge of the array manifold for accurate direction finding [6]. Many works sidestep this limitation by assuming an algebraic manifold, such as the Vandermonde steering vectors of a hypothetical uniform array with omnidirectional sensors that are perfectly isolated from each other. Obviously, such highly idealized manifolds may not be valid practice. Instead, arrays are affected by nonidealities, such as gain/phase errors [7], mutual coupling [8, 9], or sensor position perturbations [10, 11]. Calibration of the array is therefore crucial [12]. Nonidealities may nevertheless introduce ambiguities into the array manifold and decrease SNR, even after calibration, leading to excess bias and estimation error. The effective dimensionality of the measurements can also decrease, especially when the array output is intentionally compressed due to cost or hardware limitations, as in beamspace processing [1, Ch. 3.10] or hybrid beamforming [13, 14].

This work considers DoA estimation under deviations from the ideal steering matrix $\boldsymbol{A}$ of the form $\boldsymbol{CA}$, where $\boldsymbol{C}$ is a *known* matrix of nonidealities. This implies that the array is perfectly calibrated[1]. In such scenarios, $\boldsymbol{C}$ can be any complex-valued, possibly wide matrix. Consequently, it can model both compression and direction-independent perturbations. We consider the effects of such nonidealities on sparse array processing, focusing on co-array MUSIC, which can be used to find more sources than physical sensors. In particular, we propose an extension to the direct Toeplitz augmentation method [5, 15] for nonideal array manifolds. We then study the properties of this method in the infinite sample regime for a perfectly known $\boldsymbol{C}$ matrix. Our main findings are:

1. Nonidealities manifest as a signal independent additive term in the co-array covariance model. This term resembles the covariance matrix of colored noise, but is not necessarily positive semi-definite (PSD).
2. After a whitening transform, co-array MUSIC can resolve more sources than sensors perfectly, provided sufficient SNR and an infinite number of snapshots.
3. However, identifying the signal and noise subspaces may be impossible in the low SNR regime, regardless of the number of snapshots.

The paper is organized as follows. Section 2 introduces the signal model and lists the main assumptions. Section 3

[1] An uncalibrated array requires jointly estimating the nonidealities and DoAs. Consequently, $\boldsymbol{C}$ has to be constrained to a less general class of models, such as a banded Toeplitz matrix, to ensure parameter identifiability.

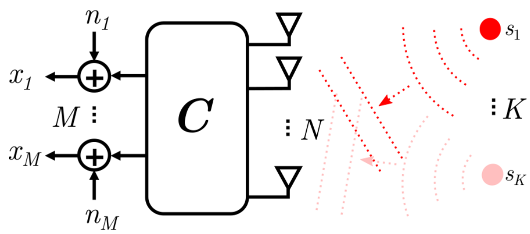

Fig. 1. Signal model. Matrix $\boldsymbol{C}$ models nonidealities due to both perturbations and compression, as $M \leq N$

Table 1. Examples of perturbation/compression matrix $\boldsymbol{C}$.

Description	Perturbation matrix model[a]	Parameters	Model relevance
Diagonal	$\boldsymbol{C} = \operatorname{diag}(\boldsymbol{g})$	$\boldsymbol{g} \in \mathbb{C}^N$	Gain/phase errors
Binary	$C_{m,n} = \mathbb{1}(i_m = n)$	$\{i_m\}_{m=1}^M \subseteq \{1, 2, \ldots, N\}$	Sensor selection
Symmetric	$C_{m,n} = \frac{c \exp(j\theta\,\lvert d_n - d_m \rvert)}{\lvert d_n - d_m \rvert + c\mathbb{1}(n=m)}$	$c \in \mathbb{C}; \theta \in (0, 2\pi]$	Mutual coupling
Phasor	$\boldsymbol{C} = \exp(j\boldsymbol{\Theta})$	$\boldsymbol{\Theta} \in (0, 2\pi]^{M \times N}$	Hybrid beamforming
Gaussian	$C_{m,n} \sim \mathcal{CN}(0, 1)$	n/a	Compressive sensing

[a] $\mathbb{1}(\cdot)$ denotes the indicator function.

briefly discusses the effect of perturbations on conventional MUSIC. Section 4 analyzes the proposed perturbation compensated co-array MUSIC algorithm. Section 5 establishes conditions under which the signal and noise subspaces are correctly identified in the inifinite snapshot regime. Finally, Section 6 concludes the paper.

2. SIGNAL MODEL

Consider K uncorrelated narrowband source signals impinging on a passive array with N sensors. The sensor outputs are subject to nonidealities modeled by matrix $\boldsymbol{C} \in \mathbb{C}^{M \times N}$, where $M \leq N$. As illustrated in Fig. 1, the M-dimensional compressed measurement vector $\boldsymbol{x} \in \mathbb{C}^M$ is modeled as

$$\boldsymbol{x} = \boldsymbol{C}\boldsymbol{A}\boldsymbol{s} + \boldsymbol{n}, \tag{1}$$

where $\boldsymbol{A} \in \mathbb{C}^{N \times K}$ is the ideal array steering matrix, $\boldsymbol{s} \in \mathbb{C}^K$ is the source signal vector, and $\boldsymbol{n} \in \mathbb{C}^M$ is a zero-mean white noise vector. Without loss of generality, we assume that $\boldsymbol{C}$ has full row rank, i.e., $\operatorname{rank}(\boldsymbol{C}) = M$. Matrix $\boldsymbol{C}$ can be interpreted as a direction-independent known matrix of nonidealities. Table 1 lists some typical cases where (1) is relevant. For example, $\boldsymbol{C}$ can model sensor gain/phase errors, hybrid beamforming, compressed sensing, or sensor selection. To a certain degree, the model can also capture mutual coupling effects in a linear array of dipole antennas, although coupling is strictly speaking an angle dependent phenomenon [6].

2.1. Covariance matrix and difference co-array

Under the uncorrelated source assumption, the covariance matrix of the measurement vector $\boldsymbol{x}$ in (1) is

$$\boldsymbol{R} \triangleq \mathbb{E}(\boldsymbol{x}\boldsymbol{x}^{\mathrm{H}}) = \boldsymbol{C}\boldsymbol{A}\boldsymbol{P}\boldsymbol{A}^{\mathrm{H}}\boldsymbol{C}^{\mathrm{H}} + \sigma^2\boldsymbol{I}, \tag{2}$$

where $\boldsymbol{P} \triangleq \mathbb{E}(\boldsymbol{s}\boldsymbol{s}^{\mathrm{H}}) = \operatorname{diag}(\boldsymbol{p})$ is a $K \times K$ diagonal matrix of positive source powers $\boldsymbol{p} = [p_1, p_2, \ldots, p_K]^{\mathrm{T}} \succ \boldsymbol{0}$, and σ^2 is the noise variance. Alternatively, (2) may be written in vectorized form as

$$\operatorname{vec}(\boldsymbol{R}) = (\boldsymbol{C}^* \otimes \boldsymbol{C})(\boldsymbol{A}^* \odot \boldsymbol{A})\boldsymbol{p} + \sigma^2 \operatorname{vec}(\boldsymbol{I}), \tag{3}$$

where $\otimes$ and $\odot$ denote the Kronecker and Khatri-Rao (columnwise Kronecker) product, respectively. The number of linearly independent equations in (3), and therefore the maximum number of resolvable sources K, is determined by the *effective steering matrix* $(\boldsymbol{C}^* \otimes \boldsymbol{C})(\boldsymbol{A}^* \odot \boldsymbol{A})$. The rank of this matrix can be of order M^2 for a sparse array, which is potentially much larger than the number of sensors N.

In particular, assuming a linear array of omnidirectional sensors at normalized positions $\mathcal{D} \triangleq \{d_n\}_{n=1}^N \subseteq \mathbb{Z}$, the entries of the ideal array steering matrix take the form

$$A_{n,k} = \exp(j2\pi d_n \delta \sin\varphi_k),$$

where $\varphi_k \in [-\pi/2, \pi/2]$ is the angle of arrival of the kth source located in the far field of the array, and δ is the unit inter-sensor spacing in wavelengths (typically $\delta = 1/2$). The entries of the effective ideal steering matrix (with $\boldsymbol{C} = \boldsymbol{I}$) thus evaluate to

$$[\boldsymbol{A}^* \odot \boldsymbol{A}]_{m+(n-1)N,k} = \exp(j2\pi(d_n - d_m)\delta \sin\varphi_k).$$

This matrix gives rise to a virtual array of sensor position differences called the difference co-array:

$$\mathcal{D}_\Delta \triangleq \mathcal{D} - \mathcal{D} = \{d_n - d_m \mid d_n, d_m \in \mathcal{D}\}.$$

The steering matrix of the difference co-array $\boldsymbol{A}_\Delta \in \mathbb{C}^{|\mathcal{D}_\Delta| \times K}$ is similarly defined as

$$[\boldsymbol{A}_\Delta]_{i,k} \triangleq \exp(j2\pi d_{\Delta,i} \delta \sin\varphi_k),$$

where $d_{\Delta,i} \in \mathcal{D}_\Delta$ are the positions of the virtual elements in the difference co-array, sorted in descending order. The effective ideal steering matrix can thus be expressed as

$$\boldsymbol{A}^* \odot \boldsymbol{A} = \boldsymbol{\Upsilon}\boldsymbol{A}_\Delta.$$

Here, an entry of the binary co-array element selection matrix $\boldsymbol{\Upsilon} \in \{0,1\}^{N^2 \times |\mathcal{D}_\Delta|}$ is ($\mathbb{1}(\cdot)$ denotes the indicator function)

$$\Upsilon_{n+(m-1)N,i} = \mathbb{1}(d_n - d_m = d_{\Delta,i}).$$

A simple counting argument shows that the number of unique virtual elements in the difference co-array satisfies $|\mathcal{D}_\Delta| \leq N(N-1)/2 \propto N^2$, which is much greater than the number of physical sensors N. The number of linearly independent equations in (3) is therefore upper bounded by $\operatorname{rank}(\boldsymbol{C})^2 = M^2 \leq N^2$, or more precisely, by the rank of matrix $(\boldsymbol{C}^* \otimes \boldsymbol{C})\boldsymbol{\Upsilon}\boldsymbol{A}_\Delta$.

2.2. Assumptions

In addition to standard assumptions, such as narrowband uncorrelated far field sources, we also assume the following:

(A1) $\boldsymbol{C}$ is known (i.e., array is calibrated or $\boldsymbol{C}$ is designed)

(A2) Exact covariance matrix is known (∞ snapshot regime)

(A3) $\mathcal{D}_\Delta$ is uniform and $\delta = 1/2$ (Nyquist condition)

(A4) $(\boldsymbol{C}^* \otimes \boldsymbol{C})\boldsymbol{\Upsilon}$ has full column rank

(A5) $\boldsymbol{H}$ is full rank (see (7) in Section 4.1 for definition)

(A1) facilitates modeling a variety of nonidealities with $\boldsymbol{C}$ (cf. Table 1). The assumption is satisfied in practice by calibrating the array. (A2) is a highly idealized assumption, but serves later to illustrate that MUSIC under known array nonidealities may suffer from subspace swap at low SNR, even in the infinite sample regime. (A3) ensures that the co-array steering matrix has Vandermonde structure, since the difference co-array assumes the form

$$\mathcal{D}_\Delta = \{-L, -L+1, \ldots, L\},$$

where $L \triangleq \max \mathcal{D} - \min \mathcal{D} \in \mathbb{N}$ is the normalized array aperture of the physical array. This guarantees that the MUSIC DoA estimates are unique and unbiased. Similarly, (A4) guarantees a Vandermonde decomposition of the virtual covariance matrix in Section 4.1, and implies that $M^2 \geq |\mathcal{D}_\Delta|$. (A5) is necessary in Section 4.2, which proposes a whitening transform for the virtual covariance matrix. Lastly, all numerical examples assume a sparse array with $M = N = 5$ sensors at normalized positions $\mathcal{D} = \{0, 1, 4, 7, 9\}$.

3. CONVENTIONAL MUSIC

In the case of fewer sources than measurements ($K < M$), MUSIC can be directly applied to the covariance matrix in (2) to estimate the DoAs. In particular, the calibrated MUSIC algorithm can be summarized in the following three steps:

Step I: Compute covariance matrix $\boldsymbol{R}$ in (2)

Step II: Find eigenvalue decomposition (EVD) of $\boldsymbol{R}$

Step III: Find zeros of null spectrum $f(\phi) = \|\boldsymbol{U}_\mathrm{n}^\mathrm{H} \boldsymbol{C}\boldsymbol{a}(\phi)\|_2$.

Here, $\boldsymbol{U}_\mathrm{n} \in \mathbb{C}^{M\times(M-K)}$ contains the eigenvectors of $\boldsymbol{R}$ spanning the noise subspace. Note that the signal and noise subspace can be identified without ambiguity, since the eigenvalues of PSD matrix $\boldsymbol{CAPA}^\mathrm{H}\boldsymbol{C}^\mathrm{H}$ are non-negative. The (perturbed) signal subspace is spanned by range space of $\boldsymbol{CA}$, which is orthogonal to the noise subspace, since $\boldsymbol{R}$ is Hermitian. Therefore, the null spectrum is zero at least for the true DoAs, i.e., $f(\phi) = 0$ when $\phi \in \{\varphi_k\}_{k=1}^K$, as shown in Fig. 2. The nulls are unique, e.g., if $\boldsymbol{Ca}$ is Vandermonde, or $\boldsymbol{a}$ is Vandermonde and $\boldsymbol{C}$ full rank. Actually, the main negative effect of the (calibrated) nonidealities is that they may cause ambiguities in the array manifold [16] and lead to false DoA estimates. They can also decrease the SNR, which increases the probability of subspace swap in the finite sample case.

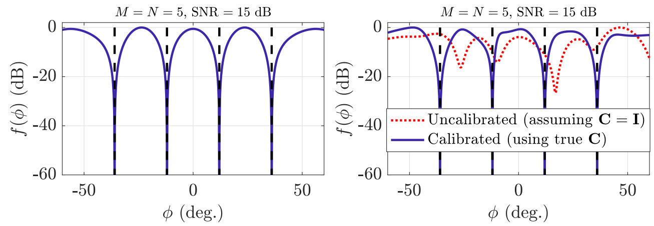

(a) Ideal case ($\boldsymbol{C} = \boldsymbol{I}$) (b) Nonideal case (Gaussian $\boldsymbol{C}$)

Fig. 2. MUSIC null spectrum. The DoAs are correctly identified after calibration, despite the nonideal array manifold.

4. CO-ARRAY MUSIC

In the case of more sources than sensors, conventional MUSIC is no longer applicable, since the $M \times M$ covariance matrix $\boldsymbol{R}$ can only be used to resolve at most $M-1 < N$ sources. However, a higher dimensional virtual covariance matrix can be constructed by leveraging the difference co-array. Essentially, such *augmented covariance* techniques lift the vectorized covariance in (3) into a matrix, whose dimensions are proportional to $|\mathcal{D}_\Delta|$. In this work, we consider *direct augmentation* [15], which is a linear mapping yielding a virtual covariance matrix with Toeplitz structure:

$$\boldsymbol{R}_\Delta \triangleq \mathcal{T}(\boldsymbol{Y}\,\mathrm{vec}(\boldsymbol{R})). \tag{4}$$

Matrix $\boldsymbol{Y} \in \mathbb{C}^{|\mathcal{D}_\Delta|\times M^2}$ maps the entries of the vectorized covariance matrix to the unique elements of the difference co-array, and $\mathcal{T}(\cdot)$ transforms the resulting vector into a Toeplitz matrix. In particular, the mth diagonal of this Toeplitz matrix equals the $(M_\Delta + |m|)$th entry of its vector argument, where

$$M_\Delta = \frac{|\mathcal{D}_\Delta| + 1}{2}$$

and $m = -(M_\Delta - 1), \ldots, M_\Delta - 1$. For example, if $\boldsymbol{C} = \boldsymbol{I}$ and $\boldsymbol{Y} = \boldsymbol{\Upsilon}^\dagger$, where $(\cdot)^\dagger$ denotes the Moore-Penrose pseudoinverse, then by (A3), Eq. (4) may be written as [15]

$$\boldsymbol{R}_\Delta = \mathcal{T}(\boldsymbol{A}_\Delta \boldsymbol{p} + \sigma^2 \boldsymbol{e}_{M_\Delta}) = \boldsymbol{ZPZ}^\mathrm{H} + \sigma^2 \boldsymbol{I}.$$

Here, $\boldsymbol{e}_{M_\Delta}$ is the standard unit vector whose M_Δth entry is unity, $\boldsymbol{P} = \mathrm{diag}(\boldsymbol{p})$ is the diagonal source power matrix in (2), and $\boldsymbol{Z} \in \mathbb{C}^{M_\Delta \times K}$ is a Vandermonde matrix. This matrix represents the steering matrix of a virtual uniform linear array with M_Δ-sensors. Applying MUSIC to $\boldsymbol{R}_\Delta$ thus enables resolving more sources than sensors, as shown in Fig. 3(a). Note that the squared matrix $\boldsymbol{R}_\Delta^2/M_\Delta$ can be interpreted as the result of applying spatial smoothing to the difference co-array using window size M_Δ [4, Theorem 2].

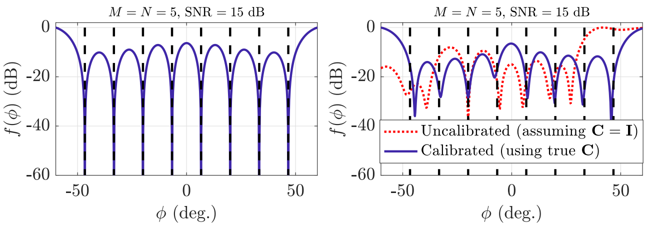

(a) Ideal case ($\boldsymbol{C} = \boldsymbol{I}$) (b) Nonideal case (Gaussian $\boldsymbol{C}$)

Fig. 3. Co-array MUSIC null spectrum. Calibrating the array enables resolving more sources than sensors, even when the array manifold is nonideal. The DoA estimates are nevertheless biased, since $\boldsymbol{H}$ is not a scaled identity matrix.

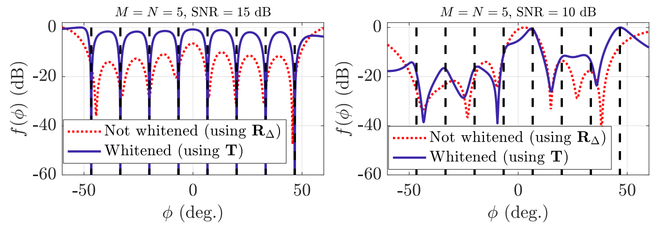

(a) High SNR (b) Low SNR

Fig. 4. Effect of diagonalizing $\boldsymbol{H}$ on co-array MUSIC. High SNR yields unbiased DoA estimates after the whitening transform in (8). Low SNR may result in excess bias and estimation error due to subspace swap or perturbation.

4.1. Covariance of calibrated virtual array

For a general $\boldsymbol{C}$ with full row rank, a natural choice for $\boldsymbol{Y}$ is

$$\boldsymbol{Y} = ((\boldsymbol{C}^* \otimes \boldsymbol{C})\boldsymbol{\Upsilon})^\dagger. \tag{5}$$

Provided (A3) and (A4) hold, (4) then reduces to

$$\boldsymbol{R}_\Delta = \boldsymbol{Z}\boldsymbol{P}\boldsymbol{Z}^\mathrm{H} + \sigma^2\boldsymbol{H}, \tag{6}$$

where $\boldsymbol{H} \in \mathbb{C}^{M_\Delta \times M_\Delta}$ is defined as

$$\boldsymbol{H} \triangleq \mathcal{T}\big((\boldsymbol{\Upsilon}^\mathrm{T}(\boldsymbol{C}^\mathrm{T}\boldsymbol{C}^* \otimes \boldsymbol{C}^\mathrm{H}\boldsymbol{C})\boldsymbol{\Upsilon})^{-1}\boldsymbol{\Upsilon}^\mathrm{T}\operatorname{vec}(\boldsymbol{C}^\mathrm{H}\boldsymbol{C})\big). \tag{7}$$

By construction, both $\boldsymbol{Z}\boldsymbol{P}\boldsymbol{Z}^\mathrm{H}$ and $\boldsymbol{H}$, and therefore also $\boldsymbol{R}_\Delta$, are Hermitian Toeplitz matrices. The Hermitian property of $\boldsymbol{H}$ follows from the symmetry of the difference co-array. In (6), $\boldsymbol{H}$ resembles the covariance matrix of colored noise. However, this interpretation is inaccurate, since $\boldsymbol{H}$ is not necessarily PSD. Indeed, $\boldsymbol{H}$ may be indefinite or even rank-deficient depending on $\boldsymbol{C}$. Nevertheless, $\boldsymbol{H}$ affects the EVD of (6) similarly to colored noise, in the sense that the signal and noise subspaces will experience perturbations. In particular, the eigenvectors of $\boldsymbol{R}_\Delta$ corresponding to the K largest magnitude eigenvalues do not necessarily span the range space of the virtual steering matrix $\boldsymbol{Z}$. The impact of this is demonstrated in Fig. 3(b), which shows the MUSIC null spectrum[2] for a random realization of $\boldsymbol{C}$. The uncalibrated (model mismatch) case incorrectly assumes $\boldsymbol{C} = \boldsymbol{I}$, whereas the calibrated case uses the correct value for $\boldsymbol{C}$. Although calibration improves the DoA esimates, these are still biased due to the subspace perturbation caused by $\boldsymbol{H}$.

4.2. Whitening transform diagonalizing $\boldsymbol{H}$

To address the subspace perturbation issue of (6), we consider the following whitening transform that diagonalizes $\boldsymbol{H}$:

$$\boldsymbol{T} \triangleq \boldsymbol{W}\boldsymbol{R}_\Delta\boldsymbol{H}^{-1}\boldsymbol{W}^{-1} = \boldsymbol{W}\boldsymbol{Z}\boldsymbol{P}\boldsymbol{Z}^\mathrm{H}\boldsymbol{H}^{-1}\boldsymbol{W}^{-1} + \sigma^2\boldsymbol{I}, \tag{8}$$

where $\boldsymbol{W} \in \mathbb{C}^{M_\Delta \times M_\Delta}$ is any full rank matrix yielding a *unitarily diagonalizable* $\boldsymbol{T}$. By the spectral theorem, $\boldsymbol{T}$ is unitarily diagonalizable if and only if it is normal, i.e., $\boldsymbol{T}^\mathrm{H}\boldsymbol{T} = \boldsymbol{T}\boldsymbol{T}^\mathrm{H}$ [17, p. 547]. E.g., if $\boldsymbol{W}$ is the eigenvector matrix of $\boldsymbol{R}_\Delta\boldsymbol{H}^{-1}$, then $\boldsymbol{T}$ is Hermitian and unitarily diagonalizable, since any Hermitian matrix is also normal. The EVD of $\boldsymbol{T}$ is

$$\boldsymbol{T} = \begin{bmatrix}\boldsymbol{U}_\mathrm{s} & \boldsymbol{U}_\mathrm{n}\end{bmatrix}\begin{bmatrix}\boldsymbol{\Lambda} + \sigma^2\boldsymbol{I} & \boldsymbol{0} \\ \boldsymbol{0} & \sigma^2\boldsymbol{I}\end{bmatrix}\begin{bmatrix}\boldsymbol{U}_\mathrm{s}^\mathrm{H} \\ \boldsymbol{U}_\mathrm{n}^\mathrm{H}\end{bmatrix}, \tag{9}$$

where $\boldsymbol{U}_\mathrm{s} \in \mathbb{C}^{M_\Delta \times K}$ and $\boldsymbol{U}_\mathrm{n} \in \mathbb{C}^{M_\Delta \times (M_\Delta - K)}$ contain the eigenvectors of $\boldsymbol{T}$, and diagonal matrix $\boldsymbol{\Lambda} \in \mathbb{R}^{K \times K}$ contains the eigenvalues of the signal component

$$\boldsymbol{W}\boldsymbol{Z}\boldsymbol{P}\boldsymbol{Z}^\mathrm{H}\boldsymbol{H}^{-1}\boldsymbol{W}^{-1} = \boldsymbol{U}_\mathrm{s}\boldsymbol{\Lambda}\boldsymbol{U}_\mathrm{s}^\mathrm{H}. \tag{10}$$

The signal and noise subspaces are orthogonal, i.e., $\boldsymbol{U}_\mathrm{s}^\mathrm{H}\boldsymbol{U}_\mathrm{n} = \boldsymbol{0}$, since matrix $[\boldsymbol{U}_\mathrm{s}\ \boldsymbol{U}_\mathrm{n}]$ is unitary. This, together with the fact that $\boldsymbol{Z}$ is Vandermonde, guarantees that the zeros in the MUSIC null spectrum

$$f(\phi) = \|\boldsymbol{U}_\mathrm{n}^\mathrm{H}\boldsymbol{W}\boldsymbol{z}(\phi)\|_2$$

uniquely correspond to the true DoAs, as shown in Fig. 4(a). Unfortunately, subspace identification based on the eigenvalues of $\boldsymbol{T}$ may be impossible, especially at low SNR, since the eigenvalue matrix $\boldsymbol{\Lambda}$ is not necessarily positive. Errors in identifying the signal and noise subspaces can lead to severe degradation of the MUSIC null spectrum, as Fig. 4(b) shows. The underlying reason for this subspace swap problem is that $\boldsymbol{H}$ is not necessarily PSD. Fig. 5 illustrates this fact using 10^4 random realizations[3] of the different $\boldsymbol{C}$ models in Table 1. A large fraction of the trials result in an indefinite $\boldsymbol{H}$, except for the diagonal and binary cases, which are always PSD (or actually, positive-definite). Note that $\boldsymbol{H}$ is never negative semi-definite, just either PSD or indefinite.

[2] $f(\phi) = \|\tilde{\boldsymbol{U}}_\mathrm{n}^\mathrm{H}\boldsymbol{z}(\phi)\|_2$, where $\tilde{\boldsymbol{U}}_\mathrm{n} \in \mathbb{C}^{M_\Delta \times (M_\Delta - K)}$ contains the eigenvectors associated with the smallest magnitude eigenvalues of $\boldsymbol{R}_\Delta$, and $\boldsymbol{z}(\phi) \in \mathbb{C}^{M_\Delta}$ is the Vandermonde steering vector in direction ϕ.

[3] With model parameters $\boldsymbol{g} \sim \mathcal{CN}(\boldsymbol{0}, \boldsymbol{I})$; $\{i_m\}_{m=1}^5 = \{m\}_{m=1}^5$; $c = 0.3e^{j\vartheta}$ and $\vartheta, \theta, \Theta_{m,n} \sim \mathcal{U}(0, 2\pi)$.

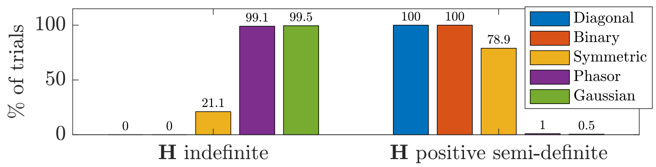

Fig. 5. Definiteness of $\boldsymbol{H}$ for random realizations of $\boldsymbol{C}$ (cf. Table 1). $\boldsymbol{H}$ is not generally PSD, but can be indefinite.

5. CONDITIONS FOR AVOIDING SUBSPACE SWAP

The correct identification of the signal and noise subspaces depends on the K signal eigenvalues

$$\tilde{\lambda}_k \triangleq \lambda_k(\boldsymbol{W}\boldsymbol{Z}\boldsymbol{P}\boldsymbol{Z}^{\mathrm{H}}\boldsymbol{H}^{-1}\boldsymbol{W}^{-1}) = \lambda_k(\boldsymbol{Z}\boldsymbol{P}\boldsymbol{Z}^{\mathrm{H}}\boldsymbol{H}^{-1}),$$

where $\lambda_k(\cdot)$ denotes the kth eigenvalue of the matrix-valued argument. Note that $\tilde{\lambda}_k$ is real, since matrices $\boldsymbol{Z}\boldsymbol{P}\boldsymbol{Z}^{\mathrm{H}}$ and $\boldsymbol{H}$ are Hermitian. If $\boldsymbol{H}$ is positive definite, then $\tilde{\lambda}_k$ is positive, and the eigenvectors associated with the K largest eigenvalue of $\boldsymbol{T}$ span the signal subspace (regardless of the SNR when the number of snapshots is infinite). However, if $\boldsymbol{H}$ is indefinite, then this is not necessarily the case. Specifically:

- If $\boldsymbol{H} \succ 0$, then $\tilde{\lambda}_k > 0\ \forall k$, which implies that $\tilde{\lambda}_k + \sigma^2 > \sigma^2\ \forall k$, i.e., subspace swap is *impossible*
- If $\boldsymbol{H}$ is indefinite, then $\exists k$ such that $\tilde{\lambda}_k < 0$, which implies that $\tilde{\lambda}_k + \sigma^2 < \sigma^2$, i.e., subspace swap is *possible*.

Associating the signal subspace with the K largest magnitude eigenvalues of $\boldsymbol{T}$, a necessary and sufficient condition for correct subspace identification is (see Fig. 6)

(C1) Subspaces correctly identified iff $|\tilde{\lambda}_k + \sigma^2| > \sigma^2\ \forall k$.

A simpler sufficient condition is

(C2) Subspaces correctly identified if $|\tilde{\lambda}_K| \geq 2\sigma^2$,

where we have assumed (without loss of generality) that the eigenvalues are sorted by magnitude in descending order, such that $\tilde{\lambda}_K$ is the smallest magnitude eigenvalue:

$$|\tilde{\lambda}_1| \geq |\tilde{\lambda}_2| \geq \ldots \geq |\tilde{\lambda}_K|.$$

Condition (C2) can also be written in terms of matrix $\boldsymbol{H}$ as:

Proposition. *Let p_K denote the weakest source power and $\lambda_K(\boldsymbol{Z}^{\mathrm{H}}\boldsymbol{Z})$ the smallest eigenvalue of matrix $\boldsymbol{Z}^{\mathrm{H}}\boldsymbol{Z}$. If*

$$\|\boldsymbol{H}\|_2 \leq \frac{1}{2}\frac{p_K}{\sigma^2}\lambda_K(\boldsymbol{Z}^{\mathrm{H}}\boldsymbol{Z}), \tag{11}$$

then the eigenvectors associated with the K largest magnitude eigenvalues of matrix $\boldsymbol{T}$ in (8) *span the signal subspace.*

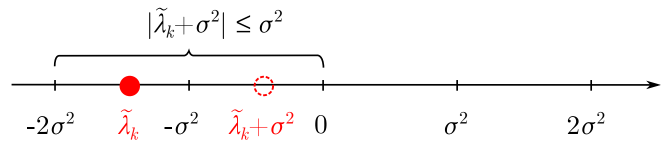

Fig. 6. Conditions for subspace swap. An eigenvalue of matrix $\boldsymbol{T}$ is incorrectly associated with the noise subspace if $-2\sigma^2 \leq \tilde{\lambda}_k \leq 0$ for some k, when the K largest magnitude eigenvalues are associated with the signal subspace.

Proof. Noting that in (10), the eigenvalue magnitudes equal the singular values, we may apply the lower bound on the smallest singular value of a matrix product [18] to arrive at

$$|\tilde{\lambda}_K| = \varsigma_K(\boldsymbol{Z}\boldsymbol{P}\boldsymbol{Z}^{\mathrm{H}}\boldsymbol{H}^{-1}) \geq \frac{\lambda_K(\boldsymbol{Z}\boldsymbol{P}\boldsymbol{Z}^{\mathrm{H}})}{\|\boldsymbol{H}\|_2}.$$

Here $\varsigma_k(\cdot)$ denotes the kth singular value. Finally, since $\boldsymbol{Z}\boldsymbol{P}\boldsymbol{Z}^{\mathrm{H}}$ is PSD, we have $\lambda_K(\boldsymbol{Z}\boldsymbol{P}\boldsymbol{Z}^{\mathrm{H}}) \geq \lambda_K(\boldsymbol{P})\lambda_K(\boldsymbol{Z}^{\mathrm{H}}\boldsymbol{Z})$, which combined with condition (C2) yields (11). □

Satisfying (11) is sufficient for identifying the signal and noise subspaces correctly, when using the eigenvalue magnitudes of the diagonalized matrix $\boldsymbol{T}$. Note that this bound is a function of the SNR of the weakest source p_K/σ^2, and the smallest eigenvalue of matrix $\boldsymbol{Z}^H\boldsymbol{Z}$, i.e., the smallest nonzero singular value of $\boldsymbol{Z}$, which in turn is a function of the source separations. Consequently, the lower the SNR or the closer the sources, the smaller the tolerated perturbation.

5.1. Sufficient condition in two source case

The upper bound in (11) simplifies significantly in the two source case. In particular, consider $K = 2$ equipower sources ($p_1 = p_2$) centered around boresight ($\varphi_1 = -\varphi_2$). Evaluating the smallest eigenvalue of the 2×2 matrix $\boldsymbol{Z}^{\mathrm{H}}\boldsymbol{Z}$ and simplifying the resulting geometric series yields

$$\|\boldsymbol{H}\|_2 \leq \frac{1}{2}\frac{p}{\sigma^2}\left(1 - \left|\frac{\sin(M_\Delta \pi \sin\varphi)}{M_\Delta \sin(\pi\sin\varphi)}\right|\right)M_\Delta. \tag{12}$$

The upper bound in (12) goes to zero as the sources approach each other ($\varphi \to 0$) for a fixed co-array size M_Δ. Conversely, if M_Δ is very large compared to the source separation, then

$$\|\boldsymbol{H}\|_2 \leq \frac{1}{2}\frac{p}{\sigma^2}M_\Delta \tag{13}$$

holds approximately. However, this does not directly imply that a larger co-array is less susceptible to subspace swap, since the dimensions of $\boldsymbol{H}$ also scale with M_Δ. A detailed investigation into the influence of the array geometry is left for future work. Finally, we note that the conditions for subspace swap of whitened matrix $\boldsymbol{T}$ are closely related to subspace perturbation bound of the unwhitened matrix $\boldsymbol{R}_\Delta$ (e.g., see [19]).

6. CONCLUSIONS

This paper studied the co-array MUSIC algorithm for calibrated arrays with angle-independent nonidealities. The considered model also applies to compressive measurements arising in, e.g., hybrid beamforming. In particular, we focused on the case of more sources than sensors in the infinite sample regime. This model sheds light on the effect of nonidealities on co-array MUSIC, which is regularly used for DoA estimation in conjunction with sparse arrays that have a uniform difference co-array. We showed that after appropriate preprocessing, the signal and noise subspaces are well defined and orthogonally separable. However, distinguishing between the two subspaces may be impossible at low SNR, regardless of the number of snapshots.

Regarding future work, a finite sample analysis of co-array MUSIC including nonidealities would be of high practical value. Another open question is whether other covariance augmentation methods (cf. [20]) are more robust to perturbations than the considered direct augmentation approach.

7. REFERENCES

[1] H. L. Van Trees, *Optimum Array Processing, Part IV of Detection, Estimation, and Modulation Theory*. Wiley-Interscience, 2002.

[2] R. Schmidt, "Multiple emitter location and signal parameter estimation," *IEEE Transactions on Antennas and Propagation*, vol. 34, no. 3, pp. 276–280, Mar 1986.

[3] P. Stoica and A. Nehorai, "MUSIC, maximum likelihood, and Cramer-Rao bound," *IEEE Transactions on Acoustics, Speech, and Signal Processing*, vol. 37, no. 5, pp. 720–741, May 1989.

[4] P. Pal and P. P. Vaidyanathan, "Nested arrays: A novel approach to array processing with enhanced degrees of freedom," *IEEE Transactions on Signal Processing*, vol. 58, no. 8, pp. 4167–4181, Aug 2010.

[5] M. Wang and A. Nehorai, "Coarrays, MUSIC, and the Cramér-Rao bound," *IEEE Transactions on Signal Processing*, vol. 65, no. 4, pp. 933–946, Feb 2017.

[6] B. Friedlander, "Antenna array manifolds for high-resolution direction finding," *IEEE Transactions on Signal Processing*, vol. 66, no. 4, pp. 923–932, 2018.

[7] ——, "A sensitivity analysis of the MUSIC algorithm," *IEEE Transactions on Acoustics, Speech, and Signal Processing*, vol. 38, no. 10, pp. 1740–1751, 1990.

[8] B. Friedlander and A. J. Weiss, "Direction finding in the presence of mutual coupling," *IEEE Transactions on Antennas and Propagation*, vol. 39, no. 3, pp. 273–284, Mar 1991.

[9] C. L. Liu and P. P. Vaidyanathan, "Super nested arrays: Linear sparse arrays with reduced mutual coupling – Part I: Fundamentals," *IEEE Transactions on Signal Processing*, vol. 64, no. 15, pp. 3997–4012, Aug 2016.

[10] A. Koochakzadeh and P. Pal, "Performance of uniform and sparse non-uniform samplers in presence of modeling errors: A Cramér-Rao bound based study," *IEEE Transactions on Signal Processing*, vol. 65, no. 6, pp. 1607–1621, 2017.

[11] M. Wang, Z. Zhang, and A. Nehorai, "Performance analysis of coarray-based MUSIC in the presence of sensor location errors," *IEEE Transactions on Signal Processing*, vol. 66, no. 12, pp. 3074–3085, June 2018.

[12] F. Belloni, A. Richter, and V. Koivunen, "Doa estimation via manifold separation for arbitrary array structures," *IEEE Transactions on Signal Processing*, vol. 55, no. 10, pp. 4800–4810, 2007.

[13] F. Sohrabi and W. Yu, "Hybrid digital and analog beamforming design for large-scale antenna arrays," *IEEE Journal of Selected Topics in Signal Processing*, vol. 10, no. 3, pp. 501–513, April 2016.

[14] A. Koochakzadeh and P. Pal, "Compressed arrays and hybrid channel sensing: A Cramér-Rao bound based analysis," *IEEE Signal Processing Letters*, vol. 27, pp. 1395–1399, 2020.

[15] C. Liu and P. P. Vaidyanathan, "Remarks on the spatial smoothing step in coarray MUSIC," *IEEE Signal Processing Letters*, vol. 22, no. 9, pp. 1438–1442, Sep. 2015.

[16] A. Manikas and C. Proukakis, "Modeling and estimation of ambiguities in linear arrays," *IEEE Transactions on Signal Processing*, vol. 46, no. 8, pp. 2166–2179, 1998.

[17] C. D. Meyer, *Matrix analysis and applied linear algebra*. Siam, 2000.

[18] B.-Y. Wang and B.-Y. Xi, "Some inequalities for singular values of matrix products," *Linear Algebra and its Applications*, vol. 264, pp. 109 – 115, 1997, sixth Special Issue on Linear Algebra and Statistics.

[19] M. C. Hücümenoğlu and P. Pal, "Effect of sparse array geometry on estimation of co-array signal subspace," in *2020 International Applied Computational Electromagnetics Society Symposium (ACES)*, 2020, pp. 1–2.

[20] A. Gorokhov, Y. Abramovich, and J. B "Unified analysis of DOA estimation algorithms for covariance matrix transforms," *Signal Processing*, vol. 55, no. 1, pp. 107 – 115, 1996.